

Title: Global patterns of forest autotrophic carbon fluxes

Running head: Global patterns of forest carbon fluxes

Authors:

Rebecca Banbury Morgan^{1,2}

Valentine Herrmann¹

Norbert Kunert^{1,3}

Ben Bond-Lamberty⁴

Helene C. Muller-Landau³

Kristina J. Anderson-Teixeira^{1,3*}

Institutional Affiliations:

1. Conservation Ecology Center; Smithsonian Conservation Biology Institute; Front Royal, VA, USA

2. School of Geography, University of Leeds, Leeds, UK

3. Center for Tropical Forest Science-Forest Global Earth Observatory; Smithsonian Tropical Research Institute; Panama, Republic of Panama

4. Joint Global Change Research Institute, Pacific Northwest National Laboratory, College Park Maryland 20740 USA

*Corresponding Author:

phone: 1-540-635-6546

fax:1-540-635-6506

email: teixeirak@si.edu

Abstract

Carbon (C) fixation, allocation, and metabolism by trees set the basis for energy and material flows in forest ecosystems and define their interactions with Earth's changing climate. However, we lack a cohesive synthesis on how forest carbon fluxes vary globally with respect to climate and one another. Here, we draw upon 1,319 records from the Global Forest Carbon Database (ForC), representing all major forest types and the nine most significant autotrophic carbon fluxes, to comprehensively explore how C cycling in mature, undisturbed forests varies with latitude and climate on a global scale. We show that, across all flux variables analyzed, C cycling decreases continuously with absolute latitude – a finding that confirms multiple previous studies but contradicts the idea that net primary productivity of temperate forests rivals that of tropical forests. C flux variables generally displayed similar trends across latitude and multiple climate variables, with no differences in allocation detected at this global scale. Temperature variables in general, and mean annual temperature and temperature seasonality in particular, were the best univariate predictors of C flux, explaining 19 - 71% of variation in the C fluxes analyzed. The effects of temperature were modified by moisture availability, with C flux reduced under hot and dry conditions and sometimes under very high precipitation. C fluxes increased with growing season length, but this was never the best univariate predictor. Within the growing season, the influence of climate on C cycling was small but significant for a number of flux variables. These findings clarify how forest C flux varies with latitude and climate on a global scale. In a period of accelerating climatic change, this improved understanding of the fundamental climatic controls on forest C cycling sets a foundation for understanding patterns of change.

Keywords: carbon fluxes; carbon dioxide (CO₂); climate; forest; global; productivity; respiration; latitude

41 Introduction

42 Carbon (C) cycling in Earth’s forests provides the energetic basis for sustaining the majority of Earth’s
43 terrestrial biodiversity and many human populations (Millennium Ecosystem Assessment, 2005), while
44 strongly influencing atmospheric carbon dioxide (CO₂) and climate (Bonan, 2008). Forests’ autotrophic
45 carbon fluxes – that is, carbon fixation, allocation, and metabolism by trees and other primary producers –
46 sets the energy ultimately available to heterotrophic organisms (including microbes), in turn influencing their
47 abundance (Niedzialkowska et al., 2010; Zak et al., 1994) and possibly diversity (Chu et al., 2018; Waide et
48 al., 1999). They are linked to cycling of energy, water, and nutrients and, critically, influence all C stocks and
49 define forest interactions with Earth’s changing climate. Each year, over 69 Gt of C cycle through Earth’s
50 forests (Badgley et al., 2019) – a flux more than seven times greater than that of recent anthropogenic fossil
51 fuel emissions (9.5 Gt C yr⁻¹; Friedlingstein et al., 2019). As atmospheric CO₂ continues to rise, driving
52 climate change, forests will play a critical role in shaping the future of Earth’s climate (Cavaleri et al., 2015;
53 Rogelj et al., 2018). However, our understanding of the climate dependence of forest C cycling on a global
54 scale has been limited by analyses typically considering only one or a few variables at a time, insufficient
55 parsing of related variables, and the mixing of data from forests that vary in stand age, disturbance history,
56 and management status, all of which affect C cycling (Gillman et al., 2015; Litton et al., 2007; Šímová &
57 Storch, 2017).

58 Forest C fluxes decrease with latitude (e.g., Luyssaert et al., 2007; Gillman et al., 2015; Li & Xiao, 2019).
59 However, studies have differed in their conclusions regarding the shape of this relationship – quite possibly
60 because of lack of standardization with respect to methodology and stand history. For instance, studies agree
61 that gross primary productivity (*GPP*) increases continuously with decreasing latitude and is indisputably
62 highest in tropical forests (Badgley et al., 2019; Beer et al., 2010; Jung et al., 2011; Li & Xiao, 2019;
63 Luyssaert et al., 2007). In contrast, some studies have suggested that net primary productivity (*NPP*), or its
64 aboveground portion (*ANPP*), exhibits a less distinct increase from temperate to tropical forests (Luyssaert
65 et al., 2007) – or even a decrease (Huston & Wolverton, 2009, but see @gillman_latitude_2015). A shallower
66 increase in *NPP* than in *GPP* with decreasing latitude would align with the suggestion that tropical forests
67 tend to have low carbon use efficiency ($CUE = NPP/GPP$; DeLucia et al., 2007; Anderson-Teixeira et
68 al., 2016; Malhi, 2012). Such differences among C fluxes their relationship to latitude could have profound
69 implications for our understanding of the C cycle and its climate sensitivity. However, until recently the
70 potential to compare latitudinal trends across C fluxes has been limited by lack of a large database with
71 standardization for methodology, stand history, and management (Anderson-Teixeira et al., 2018).

72 The latitudinal gradient in forest C flux rates, along with altitudinal gradients (Girardin et al., 2010; Malhi

et al., 2017), is driven primarily by climate, which is a significant driver of C fluxes across broad spatial scales (Cleveland et al., 2011; Luyssaert et al., 2007; Wei et al., 2010). However, there is little consensus as to the shapes of these relationships or the best predictor variables. The majority of studies have focused on exploring the relationships of C fluxes to mean annual temperature (*MAT*) and mean annual precipitation (*MAP*), as the most commonly reported site-level climate variables. C fluxes increase strongly with *MAT* on the global scale, but whether they saturate or potentially decrease at higher temperatures remains disputed. Some studies have detected no deceleration or decline in *GPP* (Luyssaert et al., 2007), *NPP* (Schoor, 2003), or root respiration (R_{root} ; Piao et al., 2010; Wei et al., 2010) with increasing *MAT*. In contrast, others have found evidence of saturation or decline of C flux in the warmest climates; Luyssaert et al. (2007) found *NPP* saturating at around 10°C *MAT*; Larjavaara & Muller-Landau (2012) found that increases in *GPP* saturate at approximately 25°C *MAT*, and Sullivan et al. (2020) found that, within the tropics, $ANPP_{stem}$ decreases at the highest maximum temperatures. C fluxes generally saturate at high levels of *MAP*, though the saturation points identified vary from *MAP* of ~1000 mm for R_{root} (Wei et al., 2010) up to 2,445 mm for *NPP* (Schoor, 2003). Interactions between *MAT* and *MAP* are also possible; within the tropics, there is a positive interaction between *MAT* and *MAP* in shaping *ANPP*, such that high rainfall has a negative effect on productivity in cooler climates, compared to a positive effect in warmer climates (Taylor et al., 2017). There is also evidence that C fluxes also respond to climate variables such as temperature and precipitation seasonality (Wagner et al., 2016), cloud cover (Taylor et al., 2017), solar radiation (Beer et al., 2010; Fyllas et al., 2017), and potential evapotranspiration (Kerkhoff et al., 2005); however, these are not typically assessed in global-scale analyses of annual forest C flux.

As metrics of annual climate, *MAT* and *MAP* fail to capture variation in climate on an intra-annual scale, including temperature and precipitation seasonality and growing season length. Some studies have suggested that the apparently strong relationship between *MAT* and C fluxes is actually a consequence of the correlation between *MAT* and growing season length (Kerkhoff et al., 2005; Michaletz et al., 2018, 2014). Kerkhoff et al. (2005) and Michaletz et al. (2014) found no significant relationship between growing season temperature and *ANPP* or *NPP* standardized to growing season length (but see Chu et al., 2016). While this suggests that the influence of temperature may be limited to determining the length of the frost-free growing season, analysis with carefully standardized variables and forest ages would be necessary to test the veracity and generality of this hypothesis.

The recent development of the Global Forest Carbon database (ForC), which synthesizes multiple variables and includes records of stand history (Anderson-Teixeira et al., 2016, 2018), opens up the possibility for a standardized analysis of global scale variation in multiple C fluxes and the principle climatic drivers of

105 these patterns. In order to approach this broad topic, we simplify the major gaps in our knowledge to five
106 broad questions and corresponding predictions (Table 1). First, we ask how nine forest autotrophic carbon
107 fluxes in ForC vary with latitude ($Q1$). We then test how these fluxes relate to MAT and MAP ($Q2$), and
108 additionally how they respond to other, less well-studied, climate variables ($Q3$). Finally, we consider the
109 relationship between C flux and seasonality, considering the role of seasonality in explaining variation in
110 carbon fluxes ($Q4$), and the influence of climate on C flux standardized by growing season length ($Q5$).

Table 1: Summary of research questions, corresponding hypotheses, and results. Statistically significant support for/ rejection of hypotheses is indicated with 'yes'/'no', and '-' indicates no significant relationship. Parentheses indicate partial overall support or rejection of hypotheses across all fluxes considered.

Questions and hypotheses	Forest autotrophic carbon fluxes										Support
	Overall	<i>GPP</i>	<i>NPP</i>	<i>ANPP</i>	<i>ANPP_{stem}</i>	<i>ANPP_{foliage}</i>	<i>BNPP</i>	<i>BNPP_{fine.root}</i>	<i>R_{auto}</i>	<i>R_{root}</i>	
Q1. How do C fluxes vary with latitude?											
C fluxes decrease continuously with latitude.	yes	yes	yes	yes	yes	yes	yes	yes	yes	yes	Fig. 2
Q2. How do C fluxes vary with mean annual temperature (MAT) and precipitation (MAP)?											
C fluxes increase continuously with MAT.	yes	yes	yes	yes	yes	yes	yes	yes	yes	yes	Figs. 3, 4, S4, S5
C fluxes increase with precipitation up to at least 2000 mm yr ⁻¹ .	yes	yes	yes	yes	yes	yes	yes	yes	yes	yes	Figs. 4, S4, S5
Temperature and precipitation jointly shape C fluxes.	(yes)	yes	yes	yes	yes	-	-	-	yes	-	Fig. 3, Table S3
Q3. How are C fluxes related to other annual climate variables?											
C fluxes display a decelerating increase or unimodal relationship with PET.	yes	yes	yes	yes	yes	yes	yes	yes	yes	yes	Figs. 4, S4, S5
C fluxes display a decelerating increase or unimodal relationship with vapour pressure deficit.	yes	yes	yes	yes	yes	yes	yes	yes	yes	yes	Figs. 4, S4, S5
C fluxes increase with solar radiation.	(yes)	yes	yes	yes	yes	yes	yes	yes	yes	-	Figs. S4, S5
Q4. How does seasonality influence annual C fluxes?											
C fluxes decrease with temperature seasonality.	yes	yes	yes	yes	yes	yes	yes	yes	yes	yes	Figs. 4, S6, S7
C fluxes decrease with precipitation seasonality.	-	-	-	-	no	-	-	-	-	-	Figs. S6, S7
C fluxes increase with growing season length.	yes	yes	yes	yes	yes	yes	yes	yes	yes	yes	Figs. 4, S6, S7
Growing season length is a better predictor of C fluxes than MAT.	(no)	no	no	no	-	no	no	no	no	no	Table S4
Q5. When standardised by growing season length, how do annual C fluxes vary with climate?											
Growing season-standardized C fluxes increase with growing season temperature.	(yes)	-	-	yes	-	yes	-	-	-	-	Figs. S8, S9
Growing season-standardized C fluxes increase with growing season PET.	(yes)	yes	yes	-	yes	-	yes	yes	-	-	Figs. S8, S9
Growing season-standardized C fluxes increase with growing season precipitation.	(yes)	-	-	yes	-	yes	-	-	-	-	Figs. S8, S9
Growing season-standardized C fluxes increase with growing season solar radiation.	(yes)	-	-	-	-	-	yes	yes	-	-	Figs. S8, S9

Materials and Methods

Forest carbon flux data

This analysis focused on nine C flux variables included in the open-access ForC database (Table 2; Anderson-Teixeira et al., 2016, 2018). ForC contains records of field-based measurements of forest carbon stocks and annual fluxes, compiled from original publications and existing data compilations and databases. Associated data, such as stand age, measurement methodologies, and disturbance history, are also included. The database was significantly expanded since the publication of Anderson-Teixeira et al. (2018) through integration with the Global Soil Respiration Database (Bond-Lamberty & Thomson, 2010). Additional targeted literature searches were conducted to identify further available data on the fluxes analyzed here, with particular focus on mature forests in temperate and boreal regions, which were not included in the review of Anderson-Teixeira et al. (2016). We used ForC v3.0, archived on Zenodo with DOI 10.5281/zenodo.3403855. This version contained 29,730 records from 4,979 plots, representing 20 distinct ecozones across all forested biogeographic and climate zones. From this, we drew 1,319 records that met our criteria, as outlined below (Fig. 1).

This analysis focused on mature forests with no known history of significant disturbance or management. There is evidence that stand age influences patterns of C flux and allocation in forest ecosystems, and can confound relationships between latitude and primary productivity (DeLucia et al., 2007; Gillman et al., 2015). To reduce any biasing effects of stand age, we included only stands of known age ≥ 100 years and those described by terms such as “mature”, “intact”, or “old-growth”. Since management can alter observed patterns of C cycling (Šímová & Storch, 2017), sites were excluded from analysis if they were managed, defined as plots that were planted, managed as plantations, irrigated, fertilised or included the term “managed” in their site description. Sites that had experienced significant disturbance within the past 100 years were also excluded. Disturbances that qualified sites for exclusion included major cutting or harvesting, burning, flooding, drought and storm events with site mortality $>10\%$ of trees. Grazed sites were retained.

Table 2: Definitions and sample sizes of carbon flux variables used in analysis. All variables are in units of $\text{Mg C ha}^{-1} \text{ yr}^{-1}$.

Variable	Definition	Components included	Methodologies	Sample size	
				records	geographic areas*
<i>GPP</i>	Gross Primary Production	full ecosystem	flux partitioning of eddy-covariance; $NPP + R_{\text{auto}}$	243	49
<i>NPP</i>	Net Primary Production	stem, foliage, coarse root, fine root, optionally others (e.g., branch, reproductive, understory)	$ANPP + BNPP$ (majority); $GPP - R_{\text{auto}}$	161	56
<i>ANPP</i>	Aboveground <i>NPP</i>	stem, foliage, optionally others (e.g., branch, reproductive, understory)	$ANPP_{\text{stem}} + ANPP_{\text{foliage}}$ (+ others)	278	86
<i>ANPP_{stem}</i>	Stem growth component of <i>ANPP</i>	woody stems down to $\text{DBH} \leq 10\text{cm}$ (no branch turnover)	stem growth measurements scaled to biomass using allometries	264	96
<i>ANPP_{foliage}</i>	Foliage component of <i>ANPP</i>	foliage	litterfall collection, with separation into components	98	49
<i>BNPP</i>	Belowground <i>NPP</i>	coarse and fine roots	coarse roots estimated indirectly using allometries based on aboveground stem increment measures ; fine roots as below	101	48
<i>BNPP_{fine.root}</i>	Fine root component of <i>BNPP</i>	fine roots	measurements combined one or more of the following: soil cores, minirhizotrons, turnover estimates, root ingrowth cores	88	41
<i>R_{auto}</i>	Autotrophic respiration	foliage, stem, and root	chamber measurements of foliage and stem gas exchange + R_{root} (as below)	22	13
<i>R_{root}</i>	Root respiration	(coarse and) fine roots	partitioning of total soil respiration (e.g., through root exclusion), scaling of root gas exchange; excluded alkali absorption and soda lime methods for measuring soil respiration	64	26

* Geographic areas group geographically proximate sites, defined using a hierarchical cluster analysis on the distance matrix of the sites, and a cutoff of 25km

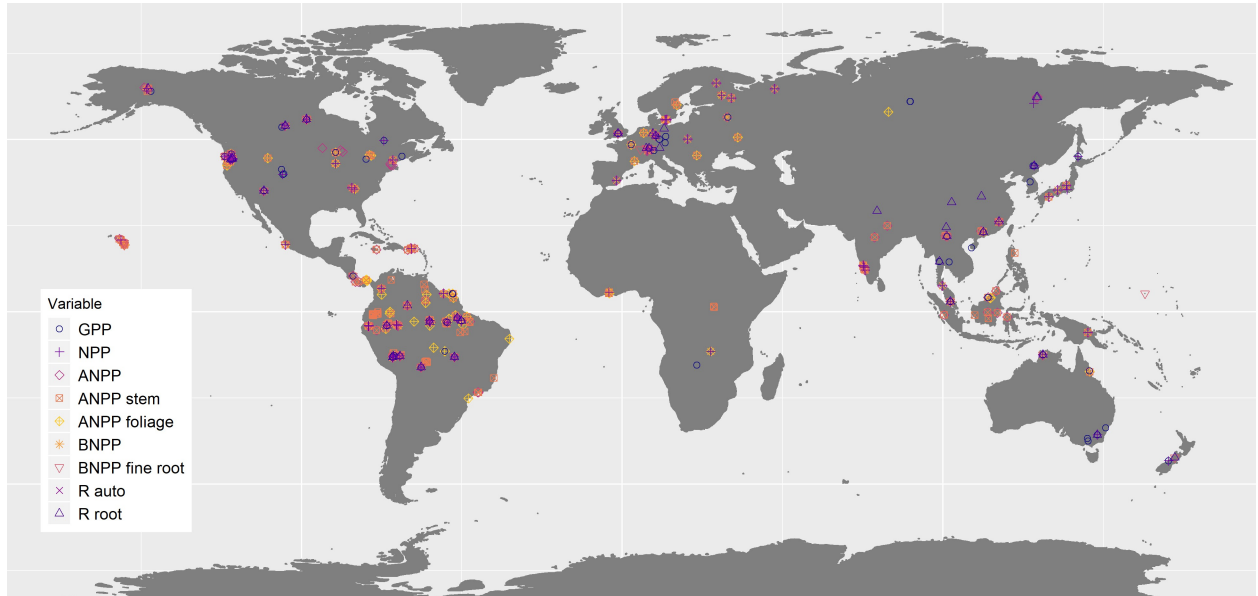


Figure 1: Map showing all data used in the analysis, coded by variable. Variables are plotted individually in Fig. S1.

Climate data

ForC contains geographic coordinates associated with each measurement record and, when available, *MAT* and *MAP* as reported in the primary literature (Anderson-Teixeira et al., 2018). Based on the geographic co-ordinates for each site, data on twelve climate variables – including *MAT*, *MAP*, temperature and precipitation seasonality, annual temperature range, solar radiation, cloud cover, annual frost and wet days, potential evapotranspiration (*PET*), aridity (*MAP/PET*), and vapor pressure deficit (*VPD*) – were extracted from five open-access climate datasets: WorldClim (Hijmans et al., 2005), WorldClim2 (Fick & Hijmans, 2017), the Climate Research Unit time-series dataset (CRU TS v4.03 (Harris et al., 2014), the Global Aridity Index and Potential Evapotranspiration Climate Database (Trabucco & Zomer, 2019), and TerraClimate (Abatzoglou et al., 2018) (Table S1). From these data, we derived maximum *VPD*, defined as the *VPD* of the month with the largest deficit, and the number of water stress months, defined as the number of months annually where precipitation was lower than *PET*. Where site-level data was missing for *MAT* or *MAP*, we used values from the WorldClim dataset.

Following the previous studies whose hypothesis we were evaluating (Kerkhoff et al., 2005; Michaletz et al., 2014), length of the growing season was estimated to the nearest month, where growing season months were defined as months with mean minimum temperature $> 0.5^{\circ}\text{C}$. We experimented with a definition of growing season months including a moisture index, defined as $(MAT - PET)/PET > -0.95$ (Kerkhoff et al., 2005; see also Michaletz et al., 2014). However, we found that including a moisture index had minimal effect on the estimates of growing season length for the sites included here, and so chose to exclude it. Monthly data for *PET*, precipitation, and temperature from CRU v 4.03 (Harris et al., 2014) and solar radiation from WorldClim2 (Fick & Hijmans, 2017) were used to calculate mean monthly *PET*, precipitation, temperature and solar radiation during the growing season.

Analyses

The effects of latitude and climate on C fluxes were analysed using mixed effects models using the package ‘lme4’ (Bates et al., 2015) in R v.3.5.1 (R Core Team, 2018). The basic model for all analyses included a fixed effect of latitude or climate and a random effect of plot nested within geographic area. Geographic areas—*i.e.*, spatially clustered sites—were defined within ForC using a hierarchical cluster analysis on the distance matrix of the sites and a cutoff of 25km (Anderson-Teixeira et al., 2018). We experimented with inclusion of altitude as a fixed effect, but excluded it from the final models because it added very little explanatory power – that is, the difference in AIC (ΔAIC) relative to models excluding altitude was generally small (often $\Delta AIC < 2$). Effects were considered significant when inclusion of the fixed effect of interest resulted in $p \leq 0.05$ and ΔAIC

165 ≥ 2.0 relative to a corresponding null model. All R^2 values presented here are marginal R^2 values, and refer
166 to the proportion of variation explained by only the fixed effects. Specific analyses are as described below.

167 We first examined the relationship between latitude and C fluxes (*Q1*; Table 1). We tested models with
168 latitude as a first-order linear, second-order polynomial, and logarithmic term. For brevity, we henceforth refer
169 to first-order linear models as “linear” and second-order polynomial models as “polynomial”. We selected as
170 the best model that with the highest Δ AIC relative to a null model with no fixed term, with the qualification
171 that a polynomial model was considered an improvement over a linear model only if it reduced the AIC value
172 by 2.0 or more.

173 To test whether trends in component fluxes across latitude sum to match those of larger fluxes, regression lines
174 for smaller component fluxes were summed to generate new estimates of larger fluxes. Because no fluxes were
175 significantly better predicted by a logarithmic or polynomial fit than by a linear fit, we used linear fits for all
176 fluxes in this analysis. We then determined whether these summed predictions fell within the 95% CI for the
177 larger flux across the entire latitudinal range. Confidence intervals for the line of best fit for the larger flux were
178 estimated using the ‘bootMer’ function, a parametric bootstrapping method for mixed models (Bates et al.,
179 2015). This function carried out 2000 simulations estimating the line of best fit, using quantiles at 0.025 and
180 0.975 to estimate 95% CIs. This analysis was applied to the following sets of fluxes: (1) $GPP = NPP + R_{auto}$,
181 (2) $NPP = ANPP + BNPP$, and (3) $ANPP = ANPP_{foliage} + ANPP_{stem}$. In addition, we estimated total
182 belowground C flux (TBCF, not analyzed due to limited data) as $TBCF = BNPP + R_{root}$.

183 Variation in allocation to component carbon fluxes was explored for three groupings: (1) $GPP = NPP + R_{auto}$,
184 (2) $NPP = ANPP + BNPP$, and (3) $ANPP = ANPP_{foliage} + ANPP_{stem}$. For each group, measurements
185 taken at the same site and plot, and in the same year, were grouped together. For groups (1) and (2), where
186 2 of the 3 flux measurements were available for a given site, plot, and year, these measurements were used
187 to calculate the third. The ratio of each pair of component fluxes was calculated. The log of these ratios
188 were regressed against latitude and climate variables, using the linear model specified above. Cook’s distance
189 analyses were carried out for each of the models, and extreme outliers removed.

190 We next examined the relationships of C fluxes to climate variables (*Q2-Q4*; Table 1). We tested first-order
191 linear, second-order polynomial, and logarithmic fits for each climate variable. Again, polynomial fits were
192 considered superior to first-order linear fits only if inclusion of a second-order polynomial term resulted in
193 $\Delta AIC \geq 2.0$ relative to a first-order linear model. We tested relationships of each C flux (Table 2) against each
194 climate variable (Table S1). Variables which were not significant explanatory variables or which explained
195 $< 20\%$ of variation in C fluxes are only presented in SI.

Multivariate models were used to investigate the potential joint and interactive effects of *MAT* and *MAP* on carbon fluxes. An additive model including *MAP* in addition to *MAT* was accepted when $\Delta\text{AIC} > 2$ relative to a null including only *MAT* as a fixed effect. An interactive model including an *MAT* x *MAP* interaction was accepted when $\Delta\text{AIC} > 2$ relative to a null including *MAT* and *MAP* as fixed effects.

To test whether and how C fluxes varied with climate when standardised by growing season length (*Q5*; Table 1), we first standardized all annual C fluxes by dividing by growing season length (as defined above). We then derived four variables to describe growing season climate, specifically growing season temperature, precipitation, solar radiation, and PET (Table S1). We tested for correlations between these standardised fluxes and growing season climate variables, using only first-order linear models.

All analyses were conducted in R v.3.5.1 (R Core Team, 2018). Code and data necessary to reproduce all results are available through GitHub (https://github.com/forc-db/Global_Productivity) and archived in Zenodo (DOI: TBD).

Results

In total, we analyzed 1,319 records from nine forest autotrophic C flux variables taken from forests that had experienced no major anthropogenic disturbances within the past 100 years. These records represented a total of 255 plots in 154 distinct geographic areas across all forested biogeographic and climate zones (Figs. 1, S1; Table 2).

Q1. How does C flux vary with latitude?

All major carbon fluxes decreased with latitude (Fig. 2; Table S2). Latitude was a strong predictor for many of the carbon fluxes, particularly the larger fluxes (Table S2). Specifically, latitude explained 64% of variation in GPP ($n = 243$, $p < 0.0001$), 50% in NPP ($n = 161$, $p < 0.0001$) and 44% in ANPP ($n = 278$, $p < 0.0001$). The C fluxes that were most poorly predicted by latitude were $BNPP_{fine.root}$ ($R^2 = 0.17$) and $ANPP_{stem}$ ($R^2 = 0.18$). The relationship with latitude was best fit by the first-order linear model, with the exception of NPP and R_{root} , for which a logarithmic model was a slightly – but not significantly – better fit.

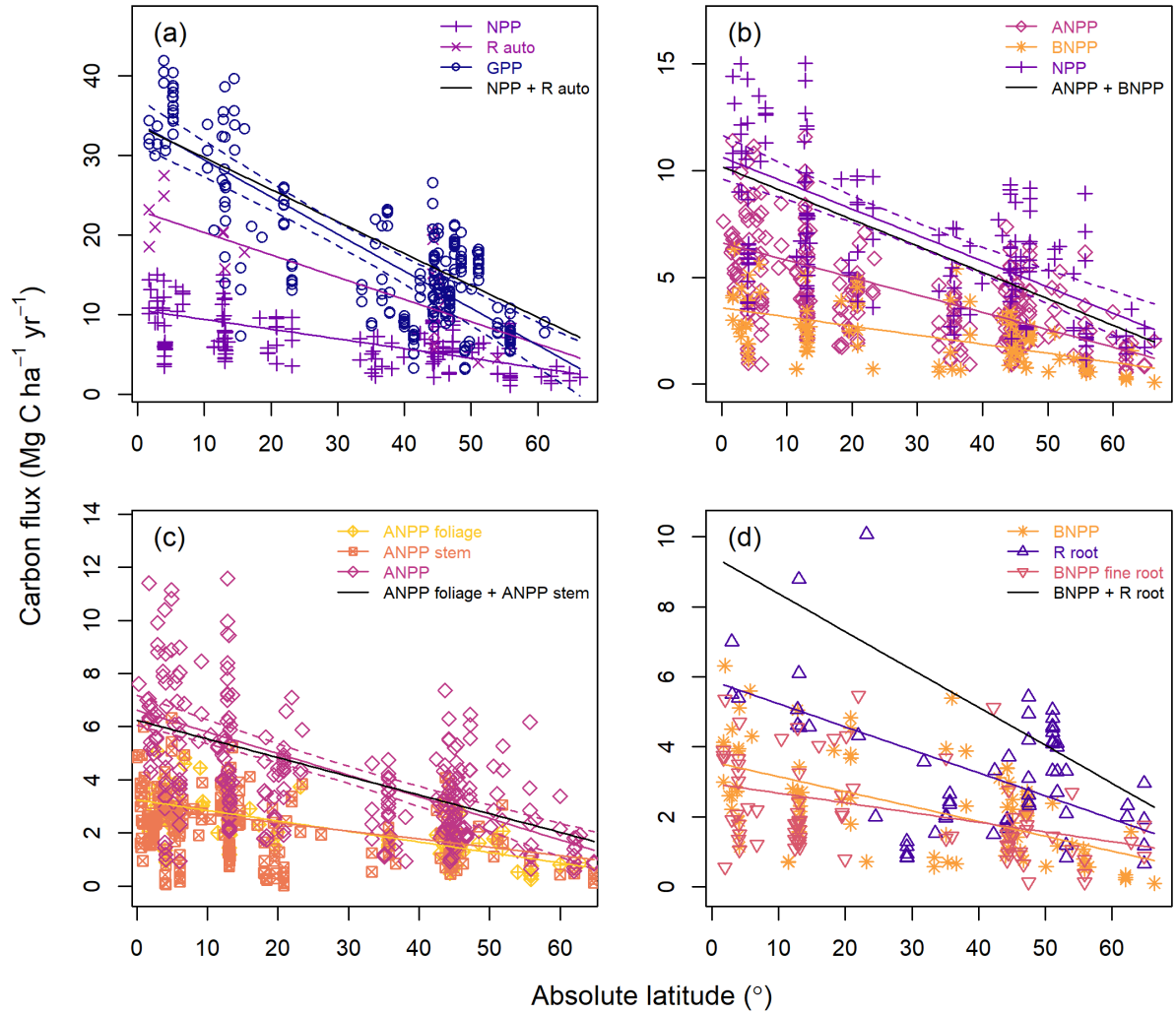


Figure 2: Latitudinal trends in forest autotrophic carbon flux. Plotted are linear models, all of which were significant ($p < 0.05$) and had AIC values within 2.0 of the best model (for two fluxes, logarithmic fits were marginally better; Table S2). Each panel shows major C fluxes together with component fluxes. Also plotted are predicted trends in the major C fluxes based on the sum of component fluxes. 95% confidence intervals are plotted for the major flux for comparison with predicted trends. In (d), which shows three belowground fluxes, the major flux, total belowground carbon flux, has insufficient data ($n=9$) to support a regression

Smaller component fluxes summed approximately to larger fluxes across the latitudinal gradient (Fig. 2). That is, modeled estimates of GPP , generated from the sum of NPP and R_{auto} ; NPP , generated from the sum of $ANPP$ and $BNPP$; and $ANPP$, generated from the sum of $ANPP_{foliage}$ and $ANPP_{stem}$, fell almost completely within the confidence intervals of the regressions of field estimates of GPP , NPP , and $ANPP$, respectively.

We found no evidence of systematic variation in C allocation with latitude or climate (Fig. S3). Of 12 relationships tested (3 ratios among C flux variables regressed against latitude, MAT , MAP and temperature

seasonality), none were significant.

Q2. How does C flux relate to MAT and MAP?

All fluxes increased with *MAT* (all $p < 0.05$; Figs. 3-4, S4-S5, Table S2). For eight of the nine fluxes, this relationship was linear. For only one variable, *BNPP*, did a lognormal fit provide an improvement over a first-order linear relationship, though this was not significant ($\Delta AIC < 2$). As with latitude, *MAT* tended to explain more variation in the larger fluxes (*GPP*, *NPP*, *ANPP*, *R_{auto}*) and *ANPP_{foliage}* (all $R^2 > 0.4$) than in subsidiary and belowground fluxes (*ANPP_{stem}*, *R_{root}*, *BNPP_{fine.root}*; all $R^2 < 0.25$).

MAP was a significant ($p < 0.05$) predictor of all fluxes (Figs. 4a, S4-S5; Table S2). However, it explained little variation: with the exception of *R_{auto}*, *MAP* explained at most 25% of variation in C flux. All fluxes increased with *MAP* up to at least 2000 mm, above which responses were variable (Figs. 4, S4-S5).

There was a significant additive effect of *MAT* and *MAP* on *GPP*, *ANPP* and *R_{auto}* (Fig. 3, Table S3), and a significant interactive effect between *MAT* and *MAP* for *NPP* and *ANPP_{stem}* (Fig. 3, Table S3). The interaction was negative for *NPP* and positive for *ANPP_{stem}*. For *ANPP_{foliage}*, *BNPP*, *BNPP_{fine.root}*, and *R_{root}*, *MAP* did not have a significant effect when accounting for *MAT* (Fig. 3, Table S3).



Figure 3: Interactive effects of mean annual temperature and precipitation on annual forest carbon fluxes. For visualization purposes, data points are grouped into bins of 0 - 1000, 1001 - 2000, 2001 - 3000, and >3000mm mean annual precipitation, and lines of best fit models are plotted for mean annual precipitation values of 500, 1500, 2500, and 3500mm. All regressions are significant ($p < 0.05$).

Q3. How does C flux relate to other annual climate variables?

All C flux variables showed a significant relationship with annual *PET*. The relationship was logarithmic for $ANPP_{foliage}$, $BNPP_{fine.root}$ and R_{root} , and polynomial for all other fluxes (Fig. 4c, S4-5; Table S2). We found strong evidence for a saturation point or peak with *PET*: C fluxes tended to increase at values below 1000mm, before saturating between 1200 and 1700mm. There was also evidence that some C fluxes begin to decrease at values above 1800mm *PET*.

Mean annual *VPD* was a significant predictor of all C fluxes. $ANPP_{foliage}$, $BNPP_{fine.root}$ and R_{root} showed

248 a logarithmic relationship with VPD , but all other fluxes showed a polynomial relationship (Figs. 4d, S4-5;
249 Table S2). C fluxes initially increased with VPD , before saturating at around 0.8 kPa, after which point
250 they began to decrease.

251 All fluxes, with the exception of R_{root} , showed a significant positive relationship with solar radiation (Figs.
252 S4-S5, Table S2). Solar radiation explained a low proportion of variability (<30%) in all C fluxes.

253 Annual wet days, cloud cover, and aridity were poor or non-significant predictors of variation in C fluxes,
254 explaining less than 20% of the variation in each of the carbon fluxes (Figs. S4-S5; Table S2).



Figure 4: Plots of carbon fluxes against (a) mean annual temperature; (b) mean annual precipitation; (c) potential evapotranspiration; (d) vapour pressure deficit; (e) temperature seasonality; (f) length of growing season. For visualization purposes, data for each flux was rescaled with a mean of 0 and standard deviation of 1. Lines of best fit are plotted according to the best model selected during analysis. All regressions are significant ($p < 0.05$).

255 *Q4. What is the role of seasonality in explaining C fluxes?*

256 Variables describing temperature seasonality – temperature seasonality, annual temperature range, annual
257 frost days, and length of growing season – were strongly correlated with both latitude and *MAT* (all $r \geq 0.2$;
258 Fig. S2), and were consistently identified as strong univariate predictors of C fluxes (Figs. 4, S4-S7).

259 All fluxes decrease with increasing temperature seasonality, though the shape of this relationship varies (all
260 $p < 0.05$; Figs. 4e, S6-7; Table S2). Temperature seasonality was strongly correlated with annual temperature
261 range, which was likewise a similarly strong predictor of C fluxes (Table S2). C fluxes were highest where
262 temperature seasonality = 0, and at an annual temperature range of 15°C or lower (*i.e.*, in the tropics).

263 In contrast, there was no significant effect of precipitation seasonality on C fluxes at this global scale. Both
264 maximum vapour pressure deficit and water stress months were poor or non-significant predictors of variation
265 in C fluxes (Figs. S6-S7; Table S2).

266 We found a significant relationship between length of growing season and C fluxes, with all fluxes showing a
267 positive relationship with length of growing season (Figs. 4e, S6-S7; Table S2). Length of growing season was
268 a strong predictor of C fluxes, explaining 53% of variation in GPP, 38% of variation in NPP, and 34% of
269 variation in ANPP (all $p < 0.05$; Table S2), but it was a weaker predictor than *MAT* for all fluxes analysed
270 (Table S4).

271 *Q5. Within the growing season, how do C fluxes vary with climate?*

272 When annual C fluxes were standardized by growing season length (in monthly increments), correlations with
273 growing season climate were generally weak (Figs. S8-S9). *ANPP* increased with growing season temperature
274 ($R^2 = 0.09$, $p < 0.001$) and precipitation ($R^2 = 0.04$, $p < 0.05$). Similarly, *ANPP_{foliage}* increased slightly with
275 growing season temperature ($R^2 = 0.16$, $p < 0.01$) and precipitation ($R^2 = 0.09$, $p < 0.05$). Growing season
276 solar radiation was positively correlated with on *BNPP* ($R^2 = 0.17$, $p < 0.001$) and *BNPP_{fine.root}* ($R^2 =$
277 0.13 , $p < 0.01$). Growing season PET had a positive influence on *GPP* ($R^2 = 0.15$, $p < 0.01$), *NPP* ($R^2 =$
278 0.07 , $p < 0.01$), *BNPP* ($R^2 = 0.23$, $p < 0.0001$), *BNPP_{fine.root}* ($R^2 = 0.10$, $p < 0.05$), and *ANPP_{stem}* ($R^2 =$
279 0.06 , $p < 0.05$). All other relationships were non-significant.

280 Discussion

281 Our analysis of a large global database (ForC) clarifies how autotrophic C fluxes in mature forests vary
282 with latitude and climate on a global scale. We show that, across all nine variables analyzed, annual C
283 flux decreases continually with latitude (Fig. 2), a finding that confirms multiple previous studies but
284 contradicts the idea that productivity of temperate forests rivals or even exceeds that of tropical forests

(Huston & Wolverton, 2009; Luyssaert et al., 2007). At this global scale, C fluxes increase approximately in proportion to one another, with component fluxes summing appropriately to larger fluxes and no detectable differences in allocation across latitude or climates (Figs. 2, 4, S3). Similarly, we show broad - *albeit* not complete - consistency of climate responses across C fluxes, with the observed latitudinal variation primarily attributable to temperature and its seasonality (Figs. 3-4). Water availability is also influential, but of secondary importance across the climate space occupied by forests (Figs. 3-4). Contrary to prior suggestions that the majority of variation in C cycling is driven primarily by the length of the growing season (Enquist et al., 2007; Kerkhoff et al., 2005; Michaletz et al., 2014), we find modest explanatory power of growing season length and small but sometimes significant influence of climate within the growing season (Figs. 4f, S6-S9). Together, these findings yield a unified understanding of climate’s influence on forest C cycling.

Our findings indicate that, among mature, undisturbed stands, forest C fluxes are unambiguously highest in the tropical regions, and the relationship with both latitude and *MAT* is approximately linear (Table 1, *Q1, Q2*; Figs. 2, 4). This contrasts with the suggestion that C fluxes (e.g., *NPP*, *ANPP*, *ANPP_{stem}*) of temperate forests are similar to or even greater than that of tropical forests (Huston & Wolverton, 2009; Luyssaert et al., 2007). Previous indications of such a pattern may have been an artifact of differences in stand age across biomes. Compared to tropical forests, the temperate forest biome has experienced more widespread anthropogenic disturbance and has a larger fraction of secondary stands (Potapov et al., 2008; Poulter et al., 2018), so analyses comparing across latitudinal gradients without controlling for stand age risk confounding age with biome effects. Because carbon allocation varies with stand age (Anderson-Teixeira et al., 2013; DeLucia et al., 2007; Doughty et al., 2018), age differences may introduce systematic biases into analyses of C fluxes across latitude or global climatic gradients. For example, woody productivity tends to be higher in rapidly aggrading secondary stands than in old-growth forests, where proportionally more C is allocated to respiration and non-woody productivity (DeLucia et al., 2007; Doughty et al., 2018; Kunert et al., 2019; Piao et al., 2010). Thus, findings that temperate forest productivity rivals that of tropical forests are likely an artifact of different forest ages across biomes.

We show that C fluxes are broadly consistent in their responses to climate drivers on the global scale, with no trends in C allocation among the variable pairs tested (Figs. 2, 4, S3). This parallels the observation that C allocation across multiple C fluxes varies little with respect to climate along a steep tropical elevational gradient (Malhi et al., 2017; but see Moser et al., 2011), and is not surprising given that carbon allocation within forest ecosystems is relatively constrained (Enquist & Niklas, 2002; Litton et al., 2007; Malhi et al., 2011). We find no trend in the allocation of *GPP* between production and respiration across latitude or climate (*NPP*:*R_{auto}*; Fig. S3), refuting the idea that tropical forests have anomalously low *CUE* (Anderson-Teixeira

et al., 2016; DeLucia et al., 2007; Malhi, 2012). Rather, differences in *CUE* between old-growth tropical forests relative to (mostly younger) extratropical forests are likely an artifact of comparing stands of different age, as *CUE* is known to decline with forest age (Collalti & Prentice, 2019; DeLucia et al., 2007; Piao et al., 2010). Another previously observed pattern for which we find no support is a tendency for belowground C allocation to decrease with increasing temperature (Gill & Finzi, 2016; Moser et al., 2011); rather, we observe no trends in allocation between *ANPP* and *BNPP* across latitudes. Failure to detect significant trends in C allocation with respect to climate in this analysis does not imply that none exist; rather, it suggests that, at this global scale, differences are subtle and/or that more careful methodological standardization is required to detect them.

Despite the broad consistency of climate responses across C fluxes, climate explains lower proportions of variability among some of the subsidiary C fluxes (*e.g.*, *ANPP_{stem}*, *BNPP*, *BNPP_{fine.root}*; Fig. 2; Tables S2, S6). There are two, non-exclusive, potential explanations for this. First, it may be that methodological variation is larger relative to flux magnitude for some of the subsidiary fluxes. Belowground fluxes in particular are difficult to quantify, and measurement methods for the belowground fluxes considered here may use fundamentally different approaches in different sites (*e.g.*, minirhizotrons, ingrowth cores, or sequential coring for *BNPP_{fine.root}*; root exclusion, stable isotope tracking, or gas exchange of excised roots for *R_{root}*), and sampling depth is variable and often insufficient to capture the full soil profile. *ANPP_{stem}*, which is also poorly explained by latitude or climate, is more straightforward to measure but is subject to variability introduced by differences such as biomass allometries applied and minimum plant size sampled (Clark et al., 2001). However, methodological variation and uncertainty affect all of fluxes considered here, and some of the larger fluxes that vary more strongly with respect to climate (*ANPP*, *NPP*) are estimated by summing uncertain component fluxes. Second, differences among variables in the proportion of variation explained by climate may be attributable to more direct climatic control over *GPP* than subsidiary fluxes. That is, subsidiary fluxes may be shaped by climate both indirectly through its influence on *GPP* and respiration and directly through any climatic influence on C allocation, as well as many other local- and regional-scale factors (*e.g.*, Moser et al., 2011).

Temperature and its seasonality were the primary drivers of C fluxes on the global scale (Table 1, *Q2, Q4*; Figs. 2-4), consistent with a long legacy of research identifying temperature as a primary driver of forest ecosystem C cycling (*e.g.*, Lieth, 1973; Luyssaert et al., 2007; Wei et al., 2010). We find little evidence of any non-linearity in temperature’s influence on C fluxes. The relationship of all fluxes to *MAT* as an individual driver were best described by a linear function (Table S2) – with the exception of *BNPP*, whose response to *MAT* was close to linear (Fig. 4a). This result contrasts with the idea that fluxes saturate with *MAT*

below approximately 25°C *MAT* (Huston & Wolverton, 2009; Luyssaert et al., 2007). It remains possible that fluxes decline above this threshold (Larjavaara & Muller-Landau, 2012; Sullivan et al., 2020), as is also consistent with tree-ring records indicating that tropical tree growth declines at high temperatures (e.g., Vlam et al., 2014). However, these higher temperatures also tend to be associated with high *PET* and *VPD*, both of which are associated with reduced C fluxes (Figs. 4c-d, S4-S5).

Indeed, while temperature responses dominate at this global scale and within the climate space occupied by forests, the effects of temperature are moderated by moisture availability (Table 1, *Q2, Q3*; Figs 3-4). Specifically, C fluxes are reduced under relatively dry conditions (*i.e.*, low *MAP*; high *VPD*) and sometimes under very high precipitation (Figs. 3-4). The observed positive interaction between *MAT* and *MAP* for *ANPP_{stem}* on the global scale (Fig. 3) is consistent with an analysis showing a similar interaction for *ANPP* in tropical forests, also with a cross-over point at ~20°C (Taylor et al., 2017).

However, we detect no such interaction for *ANPP* or most other C fluxes, and we find a contrasting negative interaction for *NPP* (Fig. 3), suggesting that more data are required to sort out potential differences in the interactive effects of *MAT* and *MAP* on C fluxes in the tropics.

Forest C fluxes decline with temperature seasonality (Table 1, *Q4*; Fig. 4e), and are minimal during cold- or dry- dormant seasons. To account for this, a number of analyses seeking to characterize global-scale effects of climate on productivity have examined the relationship of C flux per month of the growing season with growing season climatic conditions (Table 1, *Q5*; Kerkhoff et al., 2005; Anderson et al., 2006; Enquist et al., 2007; Michaletz et al., 2014). The sort of simple metric that has been used to define growing season at a global scale (Kerkhoff et al., 2005) is coarse with respect to temperature because it is calculated on a monthly timescale and problematic with respect to moisture because it doesn't capture temporal lags between precipitation and plant water use caused by storage in soil or snow. We found that a temperature-defined growing season length had strong positive correlation with C fluxes (Fig. 4f), but was never the best univariate predictor. Dividing annual fluxes by growing season length to yield average flux per growing season month removed the majority of climate-related variation, supporting the idea that the latitudinal gradient in carbon flux is attributable more to shorter growing seasons at high latitudes than to inherently lower rates of photosynthesis or respiration by high-latitude forests (Enquist et al., 2007). However, there remained a number of significant correlations with growing season climatic conditions, indicating that climatic conditions remain influential within the growing season (Figs. S8-S9). We conclude that while correcting for growing season length takes analyses a step closer to mechanistic linkage of instantaneous C flux rates to environmental conditions, it remains crude relative to the timescales on which climate affects plant metabolism, and does not advance statistical predictive power. Rather, mechanistic accounting for climatic effects on global forest carbon flux

patterns requires models representing physiologically meaningful timescales (e.g., Medvigy et al., 2009; Longo et al., 2019).

Our analysis clarifies how annual forest autotrophic C fluxes vary with latitude and climate on a global scale, with some important implications for how forest C cycling relates to climate and, by extension, how it is likely to respond to climatic warming. To the extent that patterns across broad scale climatic gradients can foretell how ecosystem responses to climate change, our findings suggest that higher temperatures with similar moisture availability would result in a generalized acceleration of forest C cycling (Figs. 2-3). This is consistent with observations of continental- to global-scale increases over time in *GPP* (Li & Xiao, 2019) and *ANPP_{stem}* (Brienen et al., 2015; Hubau et al., 2020), along with some C cycle components not considered here—tree mortality (Brienen et al., 2015; McDowell et al., 2018), soil respiration (Bond-Lamberty & Thomson, 2010), and heterotrophic soil respiration (Bond-Lamberty et al., 2018). However, increasing C flux rates are by no means universal (e.g., Rutishauser et al., 2020; Hubau et al., 2020), likely because other factors are at play, including changes to other aspects of climate, atmospheric pollution (CO_2 , SO_2 , NO_x), and local disturbances.

Moreover, forest ecosystem responses to climatic changes outside the temperature range to which forest communities are adapted and acclimatized will not necessarily parallel responses across geographic gradients in climate. Indeed, tree-ring studies from forests around the world indicate that tree growth rates – along with *ANPP_{stem}* and possibly other ecosystem C fluxes – respond negatively to temperature (Helcoski et al., 2019; Sniderhan & Baltzer, 2016). Furthermore, in the tropics, climate change will push forests beyond any contemporary climate, and there are some indications that this could reduce C flux rates (Mau et al., 2018; Sullivan et al., 2020). Further research is required to understand the extent to which forest responses to climate change will track the observed global gradients, and the time scale on which they will do so. In the meantime, understanding the fundamental climatic controls on annual C cycling in Earth’s forests sets a firmer foundation for understanding forest C cycle responses to accelerating climate change.

Acknowledgements

We gratefully acknowledge all authors of the original studies and data compilations included in this analysis, their funding agencies, and the various networks that support ground-based measurements of C fluxes. We also thank the numerous researchers who have contributed to the building of ForC. This study was funded by a Smithsonian Scholarly Studies grant to KJAT and HCML and by Smithsonian’s Forest Global Earth Observatory (ForestGEO). Original compilation of the ForC database was funded by DOE grants DE-SC0008085 and DE-SC0010039 to KAT.

References

- Abatzoglou, J. T., Dobrowski, S. Z., Parks, S. A., & Hegewisch, K. C. (2018). TerraClimate, a high-resolution global dataset of monthly climate and climatic water balance from 1958–2015. *Scientific Data*, 5(1), 170191. <https://doi.org/10.1038/sdata.2017.191>
- Anderson, K. J., Allen, A. P., Gillooly, J. F., & Brown, J. H. (2006). Temperature-dependence of biomass accumulation rates during secondary succession. *Ecology Letters*, 9(6), 673–682. <https://doi.org/10.1111/j.1461-0248.2006.00914.x>
- Anderson-Teixeira, K. J., Miller, A. D., Mohan, J. E., Hudiburg, T. W., Duval, B. D., & DeLucia, E. H. (2013). Altered dynamics of forest recovery under a changing climate. *Global Change Biology*, 19(7), 2001–2021. <https://doi.org/10.1111/gcb.12194>
- Anderson-Teixeira, K. J., Wang, M. M. H., McGarvey, J. C., Herrmann, V., Tepley, A. J., Bond-Lamberty, B., & LeBauer, D. S. (2018). ForC: A global database of forest carbon stocks and fluxes. *Ecology*, 99(6), 1507–1507. <https://doi.org/10.1002/ecy.2229>
- Anderson-Teixeira, K. J., Wang, M. M. H., McGarvey, J. C., & LeBauer, D. S. (2016). Carbon dynamics of mature and regrowth tropical forests derived from a pantropical database (TropForC-db). *Global Change Biology*, 22(5), 1690–1709. <https://doi.org/10.1111/gcb.13226>
- Badgley, G., Anderegg, L. D. L., Berry, J. A., & Field, C. B. (2019). Terrestrial gross primary production: Using NIR_v to scale from site to globe. *Global Change Biology*, 25(11), 3731–3740. <https://doi.org/10.1111/gcb.14729>
- Bates, D., Mächler, M., Bolker, B., & Walker, S. (2015). Fitting Linear Mixed-Effects Models Using **lme4**. *Journal of Statistical Software*, 67(1). <https://doi.org/10.18637/jss.v067.i01>
- Beer, C., Reichstein, M., Tomelleri, E., Ciais, P., Jung, M., Carvalhais, N., Rodenbeck, C., Arain, M. A., Baldocchi, D., Bonan, G. B., Bondeau, A., Cescatti, A., Lasslop, G., Lindroth, A., Lomas, M., Luyssaert, S., Margolis, H., Oleson, K. W., Rouspard, O., ... Papale, D. (2010). Terrestrial Gross Carbon Dioxide Uptake: Global Distribution and Covariation with Climate. *Science*, 329(5993), 834–838. <https://doi.org/10.1126/science.1184984>
- Bonan, G. B. (2008). Forests and Climate Change: Forcings, Feedbacks, and the Climate Benefits of Forests. *Science*, 320(5882), 1444–1449. <https://doi.org/10.1126/science.1155121>
- Bond-Lamberty, B., Bailey, V. L., Chen, M., Gough, C. M., & Vargas, R. (2018). Globally rising soil

heterotrophic respiration over recent decades. *Nature*, 560(7716), 80–83. <https://doi.org/10.1038/s41586-018-0358-x>

Bond-Lamberty, B., & Thomson, A. (2010). A global database of soil respiration data. *Biogeosciences*, 7(6), 1915–1926. <https://doi.org/10.5194/bg-7-1915-2010>

Brienen, R. J. W., Phillips, O. L., Feldpausch, T. R., Gloor, E., Baker, T. R., Lloyd, J., Lopez-Gonzalez, G., Monteagudo-Mendoza, A., Malhi, Y., Lewis, S. L., Vásquez Martinez, R., Alexiades, M., Álvarez Dávila, E., Alvarez-Loayza, P., Andrade, A., Aragão, L. E. O. C., Araujo-Murakami, A., Arets, E. J. M. M., Arroyo, L., ... Zagt, R. J. (2015). Long-term decline of the Amazon carbon sink. *Nature*, 519(7543), 344–348. <https://doi.org/10.1038/nature14283>

Cavaleri, M. A., Reed, S. C., Smith, W. K., & Wood, T. E. (2015). Urgent need for warming experiments in tropical forests. *Global Change Biology*, 21(6), 2111–2121. <https://doi.org/10.1111/gcb.12860>

Chu, C., Bartlett, M., Wang, Y., He, F., Weiner, J., Chave, J., & Sack, L. (2016). Does climate directly influence NPP globally? *Global Change Biology*, 22(1), 12–24. <https://doi.org/10.1111/gcb.13079>

Chu, C., Lutz, J. A., Král, K., Vrška, T., Yin, X., Myers, J. A., Abiem, I., Alonso, A., Bourg, N., Burslem, D. F. R. P., Cao, M., Chapman, H., Condit, R., Fang, S., Fischer, G. A., Gao, L., Hao, Z., Hau, B. C. H., He, Q., ... He, F. (2018). Direct and indirect effects of climate on richness drive the latitudinal diversity gradient in forest trees. *Ecology Letters*, ele.13175. <https://doi.org/10.1111/ele.13175>

Clark, D. A., Brown, S., Kicklighter, D. W., Chambers, J. Q., Thomlinson, J. R., & Ni, J. (2001). Measuring net primary production in forests: Concepts and field methods. *Ecological Applications*, 11(2), 15.

Cleveland, C. C., Townsend, A. R., Taylor, P., Alvarez-Clare, S., Bustamante, M. M. C., Chuyong, G., Dobrowski, S. Z., Grierson, P., Harms, K. E., Houlton, B. Z., Marklein, A., Parton, W., Porder, S., Reed, S. C., Sierra, C. A., Silver, W. L., Tanner, E. V. J., & Wieder, W. R. (2011). Relationships among net primary productivity, nutrients and climate in tropical rain forest: A pan-tropical analysis: Nutrients, climate and tropical NPP. *Ecology Letters*, 14(9), 939–947. <https://doi.org/10.1111/j.1461-0248.2011.01658.x>

Collalti, A., & Prentice, I. C. (2019). Is NPP proportional to GPP? Waring’s hypothesis 20 years on. *Tree Physiology*, 39(8), 1473–1483. <https://doi.org/10.1093/treephys/tpz034>

DeLucia, E. H., Drake, J. E., Thomas, R. B., & Gonzalez-Meler, M. (2007). Forest carbon use efficiency: Is respiration a constant fraction of gross primary production? *Global Change Biology*, 13(6), 1157–1167. <https://doi.org/10.1111/j.1365-2486.2007.01365.x>

Doughty, C. E., Goldsmith, G. R., Raab, N., Girardin, C. A. J., Farfan-Amezquita, F., Huaraca-Huasco, W.,

471 Silva-Espejo, J. E., Araujo-Murakami, A., Costa, A. C. L. da, Rocha, W., Galbraith, D., Meir, P., Metcalfe,
472 D. B., & Malhi, Y. (2018). What controls variation in carbon use efficiency among Amazonian tropical
473 forests? *Biotropica*, 50(1), 16–25. <https://doi.org/10.1111/btp.12504>

474 Enquist, B. J., Kerkhoff, A. J., Huxman, T. E., & Economo, E. P. (2007). Adaptive differences in plant
475 physiology and ecosystem paradoxes: Insights from metabolic scaling theory. *Global Change Biology*, 13(3),
476 591–609. <https://doi.org/10.1111/j.1365-2486.2006.01222.x>

477 Enquist, B. J., & Niklas, K. J. (2002). Global Allocation Rules for Patterns of Biomass Partitioning in Seed
478 Plants. *Science*, 295(5559), 1517–1520. <https://doi.org/10.1126/science.1066360>

479 Fick, S. E., & Hijmans, R. J. (2017). WorldClim 2: New 1-km spatial resolution climate surfaces for
480 global land areas: New climate surfaces for global land areas. *International Journal of Climatology*, 37(12),
481 4302–4315. <https://doi.org/10.1002/joc.5086>

482 Friedlingstein, P., Jones, M. W., O’Sullivan, M., Andrew, R. M., Hauck, J., Peters, G. P., Peters, W.,
483 Pongratz, J., Sitch, S., Quéré, C. L., Bakker, D. C. E., Canadell, J. G., Ciais, P., Jackson, R. B., Anthoni, P.,
484 Barbero, L., Bastos, A., Bastrikov, V., Becker, M., ... Zaehle, S. (2019). Global Carbon Budget 2019. *Earth*
485 *System Science Data*, 11(4), 1783–1838. <https://doi.org/https://doi.org/10.5194/essd-11-1783-2019>

486 Fyllas, N. M., Bentley, L. P., Shenkin, A., Asner, G. P., Atkin, O. K., Díaz, S., Enquist, B. J., Farfan-Rios,
487 W., Gloor, E., Guerrieri, R., Huasco, W. H., Ishida, Y., Martin, R. E., Meir, P., Phillips, O., Salinas, N.,
488 Silman, M., Weerasinghe, L. K., Zaragoza-Castells, J., & Malhi, Y. (2017). Solar radiation and functional
489 traits explain the decline of forest primary productivity along a tropical elevation gradient. *Ecology Letters*,
490 20(6), 730–740. <https://doi.org/10.1111/ele.12771>

491 Gill, A. L., & Finzi, A. C. (2016). Belowground carbon flux links biogeochemical cycles and resource-use
492 efficiency at the global scale. *Ecology Letters*, 19(12), 1419–1428. <https://doi.org/10.1111/ele.12690>

493 Gillman, L. N., Wright, S. D., Cusens, J., McBride, P. D., Malhi, Y., & Whittaker, R. J. (2015). Latitude,
494 productivity and species richness: Latitude and productivity. *Global Ecology and Biogeography*, 24(1),
495 107–117. <https://doi.org/10.1111/geb.12245>

496 Girardin, C. A. J., Malhi, Y., Aragão, L. E. O. C., Mamani, M., Huaraca Huasco, W., Durand, L., Feeley, K.
497 J., Rapp, J., Silva-Espejo, J. E., Silman, M., Salinas, N., & Whittaker, R. J. (2010). Net primary productivity
498 allocation and cycling of carbon along a tropical forest elevational transect in the Peruvian Andes. *Global*
499 *Change Biology*, 16(12), 3176–3192. <https://doi.org/10.1111/j.1365-2486.2010.02235.x>

500 Harris, I., Jones, P. D., Osborn, T. J., & Lister, D. H. (2014). Updated high-resolution grids of monthly climatic

501 observations - the CRU TS3.10 Dataset: Updated high-resolution grids of monthly climatic observations.
 502 *International Journal of Climatology*, 34(3), 623–642. <https://doi.org/10.1002/joc.3711>

503 Helcoski, R., Tepley, A. J., Pederson, N., McGarvey, J. C., Meakem, V., Herrmann, V., Thompson, J. R., &
 504 Anderson-Teixeira, K. J. (2019). Growing season moisture drives interannual variation in woody productivity
 505 of a temperate deciduous forest. *New Phytologist*, 223(3), 1204–1216. <https://doi.org/10.1111/nph.15906>

506 Hijmans, R. J., Cameron, S. E., Parra, J. L., Jones, P. G., & Jarvis, A. (2005). Very high resolution
 507 interpolated climate surfaces for global land areas. *International Journal of Climatology*, 25(15), 1965–1978.
 508 <https://doi.org/10.1002/joc.1276>

509 Hubau, W., Lewis, S. L., Phillips, O. L., Affum-Baffoe, K., Beeckman, H., Cuní-Sanchez, A., Daniels, A. K.,
 510 Ewango, C. E. N., Fauset, S., Mukinzi, J. M., Sheil, D., Sonké, B., Sullivan, M. J. P., Sunderland, T. C. H.,
 511 Taedoung, H., Thomas, S. C., White, L. J. T., Abernethy, K. A., Adu-Bredu, S., ... Zemagho, L. (2020).
 512 Asynchronous carbon sink saturation in African and Amazonian tropical forests. *Nature*, 579(7797), 80–87.
 513 <https://doi.org/10.1038/s41586-020-2035-0>

514 Huston, M. A., & Wolverton, S. (2009). The global distribution of net primary production: Resolving the
 515 paradox. *Ecological Monographs*, 79(3), 343–377. <https://doi.org/10.1890/08-0588.1>

516 Jung, M., Reichstein, M., Margolis, H. A., Cescatti, A., Richardson, A. D., Arain, M. A., Arneeth, A.,
 517 Bernhofer, C., Bonal, D., Chen, J., Gianelle, D., Gobron, N., Kiely, G., Kutsch, W., Lasslop, G., Law, B. E.,
 518 Lindroth, A., Merbold, L., Montagnani, L., ... Williams, C. (2011). Global patterns of land-atmosphere fluxes
 519 of carbon dioxide, latent heat, and sensible heat derived from eddy covariance, satellite, and meteorological
 520 observations. *Journal of Geophysical Research*, 116, G00J07. <https://doi.org/10.1029/2010JG001566>

521 Kerkhoff, A. J., Enquist, B. J., Elser, J. J., & Fagan, W. F. (2005). Plant allometry, stoichiometry and the
 522 temperature-dependence of primary productivity: Plant allometry, stoichiometry and productivity. *Global*
 523 *Ecology and Biogeography*, 14(6), 585–598. <https://doi.org/10.1111/j.1466-822X.2005.00187.x>

524 Kunert, N., El-Madany, T. S., Aparecido, L. M. T., Wolf, S., & Potvin, C. (2019). Understanding the controls
 525 over forest carbon use efficiency on small spatial scales: Effects of forest disturbance and tree diversity.
 526 *Agricultural and Forest Meteorology*, 269–270, 136–144. <https://doi.org/10.1016/j.agrformet.2019.02.007>

527 Larjavaara, M., & Muller-Landau, H. C. (2012). Temperature explains global variation in biomass among
 528 humid old-growth forests: Temperature and old-growth forest biomass. *Global Ecology and Biogeography*,
 529 21(10), 998–1006. <https://doi.org/10.1111/j.1466-8238.2011.00740.x>

530 Lieth, H. (1973). Primary production: Terrestrial ecosystems. *Human Ecology*, 1(4), 303–332. <https://doi.org/10.1007/BF01531013>

531 //doi.org/10.1007/BF01536729

532 Litton, C. M., Raich, J. W., & Ryan, M. G. (2007). Carbon allocation in forest ecosystems. *Global Change*
533 *Biology*, 13(10), 2089–2109. <https://doi.org/10.1111/j.1365-2486.2007.01420.x>

534 Li, & Xiao. (2019). Mapping Photosynthesis Solely from Solar-Induced Chlorophyll Fluorescence: A Global,
535 Fine-Resolution Dataset of Gross Primary Production Derived from OCO-2. *Remote Sensing*, 11(21), 2563.
536 <https://doi.org/10.3390/rs11212563>

537 Longo, M., Knox, R. G., Medvigy, D. M., Levine, N. M., Dietze, M. C., Kim, Y., Swann, A. L. S., Zhang,
538 K., Rollinson, C. R., Bras, R. L., Wofsy, S. C., & Moorcroft, P. R. (2019). The biophysics, ecology, and
539 biogeochemistry of functionally diverse, vertically and horizontally heterogeneous ecosystems: The Ecosystem
540 Demography model, version 2.2 – Part 1: Model description. *Geoscientific Model Development*, 12(10),
541 4309–4346. <https://doi.org/10.5194/gmd-12-4309-2019>

542 Luyssaert, S., Inglima, I., Jung, M., Richardson, A. D., Reichstein, M., Papale, D., Piao, S. L., Schulze,
543 E. D., Wingate, L., Matteucci, G., Aragao, L., Aubinet, M., Beer, C., Bernhofer, C., Black, K. G., Bonal,
544 D., Bonnefond, J. M., Chambers, J., Ciais, P., ... Janssens, I. A. (2007). CO₂ balance of boreal,
545 temperate, and tropical forests derived from a global database. *Global Change Biology*, 13(12), 2509–2537.
546 <https://doi.org/10.1111/j.1365-2486.2007.01439.x>

547 Malhi, Y. (2012). The productivity, metabolism and carbon cycle of tropical forest vegetation: Carbon cycle
548 of tropical forests. *Journal of Ecology*, 100(1), 65–75. <https://doi.org/10.1111/j.1365-2745.2011.01916.x>

549 Malhi, Y., Doughty, C., & Galbraith, D. (2011). The allocation of ecosystem net primary productivity in
550 tropical forests. *Philosophical Transactions of the Royal Society B: Biological Sciences*, 366(1582), 3225–3245.
551 <https://doi.org/10.1098/rstb.2011.0062>

552 Malhi, Y., Girardin, C. A. J., Goldsmith, G. R., Doughty, C. E., Salinas, N., Metcalfe, D. B., Huaraca Huasco,
553 W., Silva-Espejo, J. E., Aguilla-Pasquell, J. del, Farfán Amézquita, F., Aragão, L. E. O. C., Guerrieri, R.,
554 Ishida, F. Y., Bahar, N. H. A., Farfan-Rios, W., Phillips, O. L., Meir, P., & Silman, M. (2017). The variation
555 of productivity and its allocation along a tropical elevation gradient: A whole carbon budget perspective.
556 *New Phytologist*, 214(3), 1019–1032. <https://doi.org/10.1111/nph.14189>

557 Mau, A., Reed, S., Wood, T., & Cavaleri, M. (2018). Temperate and Tropical Forest Canopies are Already
558 Functioning beyond Their Thermal Thresholds for Photosynthesis. *Forests*, 9(1), 47. <https://doi.org/10.3390/f9010047>

559 0/f9010047

560 McDowell, N., Allen, C. D., Anderson-Teixeira, K., Brando, P., Brien, R., Chambers, J., Christoffersen, B.,

Davies, S., Doughty, C., Duque, A., Espirito-Santo, F., Fisher, R., Fontes, C. G., Galbraith, D., Goodsman,
 D., Grossiord, C., Hartmann, H., Holm, J., Johnson, D. J., ... Xu, X. (2018). Drivers and mechanisms of
 tree mortality in moist tropical forests. *New Phytologist*, 219(3), 851–869. <https://doi.org/10.1111/nph.15027>
 Medvigy, D., Wofsy, S. C., Munger, J. W., Hollinger, D. Y., & Moorcroft, P. R. (2009). Mechanistic scaling
 of ecosystem function and dynamics in space and time: Ecosystem Demography model version 2. *Journal of*
Geophysical Research: Biogeosciences, 114(G1), G01002. <https://doi.org/10.1029/2008JG000812>
 Michaletz, S. T., Cheng, D., Kerkhoff, A. J., & Enquist, B. J. (2014). Convergence of terrestrial plant
 production across global climate gradients. *Nature*, 512(7512), 39–43. <https://doi.org/10.1038/nature13470>
 Michaletz, S. T., Kerkhoff, A. J., & Enquist, B. J. (2018). Drivers of terrestrial plant production across broad
 geographical gradients. *Global Ecology and Biogeography*, 27(2), 166–174. <https://doi.org/10.1111/geb.12685>
 Millennium Ecosystem Assessment. (2005). *Ecosystems and Human Well-being: Synthesis*. Island Press.
 Moser, G., Leuschner, C., Hertel, D., Graefe, S., Soethe, N., & Iost, S. (2011). Elevation effects on the carbon
 budget of tropical mountain forests (S Ecuador): The role of the belowground compartment. *Global Change*
Biology, 17(6), 2211–2226. <https://doi.org/10.1111/j.1365-2486.2010.02367.x>
 Niedziałkowska, M., Kończak, J., Czarnomska, S., & Jędrzejewska, B. (2010). Species diversity and
 abundance of small mammals in relation to forest productivity in northeast Poland. *Écoscience*, 17(1),
 109–119. <https://doi.org/10.2980/17-1-3310>
 Piao, S., Luyssaert, S., Ciais, P., Janssens, I. A., Chen, A., Cao, C., Fang, J., Friedlingstein, P., Luo, Y.,
 & Wang, S. (2010). Forest annual carbon cost: A global-scale analysis of autotrophic respiration. *Ecology*,
 91(3), 652–661. <https://doi.org/10.1890/08-2176.1>
 Potapov, P., Yaroshenko, A., Turubanova, S., Dubinin, M., Laestadius, L., Thies, C., Aksenov, D., Egorov,
 A., Yesipova, Y., Glushkov, I., Karpachevskiy, M., Kostikova, A., Manisha, A., Tsybikova, E., & Zhuravleva,
 I. (2008). Mapping the World's Intact Forest Landscapes by Remote Sensing. *Ecology and Society*, 13(2),
 art51. <https://doi.org/10.5751/ES-02670-130251>
 Poulter, B., Aragao, L., Andela, N., Bellassen, V., Ciais, P., Kato, T., Lin, X., Nachin, B., Luyssaert, S.,
 Pederson, N., Peylin, P., Piao, S., Saatchi, S., Schepaschenko, D., Schelhaas, M., & Shvidenko, A. (2018).
The global forest age dataset (GFADv1.0), link to NetCDF file. PANGAEA. <https://doi.org/10.1594/PANGAEA.889943>
 R Core Team. (2018). *R: A language and environment for statistical computing*. R Foundation for Statistical
 Computing. <https://www.R-project.org>

591 Rogelj, J., Shindell, D., Jiang, K., Ffifita, S., Forster, P., Ginzburg, V., Handa, C., Kobayashi, S., Kriegler, E.,
592 Mundaca, L., Séférian, R., Vilariño, M. V., Calvin, K., Emmerling, J., Fuss, S., Gillett, N., He, C., Hertwich,
593 E., Höglund-Isaksson, L., ... Schaeffer, R. (2018). *Mitigation Pathways Compatible with 1.5°C in the Context*
594 *of Sustainable Development*. 82.

595 Rutishauser, E., Wright, S. J., Condit, R., Hubbell, S. P., Davies, S. J., & Muller-Landau, H. C. (2020). Testing
596 for changes in biomass dynamics in large-scale forest datasets. *Global Change Biology*, 26(3), 1485–1498.
597 <https://doi.org/10.1111/gcb.14833>

598 Schuur, E. A. G. (2003). Productivity and global climate revisited: The sensitivity of tropical forest growth
599 to precipitation. *Ecology*, 84(5), 1165–1170. [https://doi.org/10.1890/0012-9658\(2003\)084%5B1165:](https://doi.org/10.1890/0012-9658(2003)084%5B1165:PAGCRT%5D2.0.CO;2)
600 [PAGCRT%5D2.0.CO;2](https://doi.org/10.1890/0012-9658(2003)084%5B1165:PAGCRT%5D2.0.CO;2)

601 Sniderhan, A. E., & Baltzer, J. L. (2016). Growth dynamics of black spruce (*Picea mariana*) in a rapidly
602 thawing discontinuous permafrost peatland: Growth Dynamics Boreal Peatlands. *Journal of Geophysical*
603 *Research: Biogeosciences*, 121(12), 2988–3000. <https://doi.org/10.1002/2016JG003528>

604 Sullivan, M. J. P., Lewis, S. L., Affum-Baffoe, K., Castilho, C., Costa, F., Sanchez, A. C., Ewango, C. E. N.,
605 Hubau, W., Marimon, B., Monteagudo-Mendoza, A., Qie, L., Sonké, B., Martinez, R. V., Baker, T. R., Brien, R. J. W.,
606 Feldpausch, T. R., Galbraith, D., Gloor, M., Malhi, Y., ... Phillips, O. L. (2020). Long-term thermal
607 sensitivity of Earth’s tropical forests. *Science*, 368(6493), 869–874. <https://doi.org/10.1126/science.aaw7578>

608 Šimová, I., & Storch, D. (2017). The enigma of terrestrial primary productivity: Measurements, models, scales
609 and the diversity-productivity relationship. *Ecography*, 40(2), 239–252. <https://doi.org/10.1111/ecog.02482>

610 Taylor, P. G., Cleveland, C. C., Wieder, W. R., Sullivan, B. W., Doughty, C. E., Dobrowski, S. Z., &
611 Townsend, A. R. (2017). Temperature and rainfall interact to control carbon cycling in tropical forests.
612 *Ecology Letters*, 20(6), 779–788. <https://doi.org/10.1111/ele.12765>

613 Trabucco, A., & Zomer, R. J. (2019). *Global Aridity Index and Potential Evapo-Transpiration (ET0) Climate*
614 *Database v2*. 10. <https://doi.org/10.6084/m9.figshare.7504448.v3>

615 Vlam, M., Baker, P. J., Bunyavejchewin, S., & Zuidema, P. A. (2014). Temperature and rainfall strongly
616 drive temporal growth variation in Asian tropical forest trees. *Oecologia*, 174(4), 1449–1461. <https://doi.org/10.1007/s00442-013-2846-x>

617 Wagner, F. H., Hérault, B., Bonal, D., Stahl, C., Anderson, L. O., Baker, T. R., Becker, G. S., Beeckman, H.,
618 Boanerges Souza, D., Botosso, P. C., Bowman, D. M. J. S., Bräuning, A., Brede, B., Brown, F. I., Camarero,
619 J. J., Camargo, P. B., Cardoso, F. C. G., Carvalho, F. A., Castro, W., ... Aragão, L. E. O. C. (2016).

621 Climate seasonality limits leaf carbon assimilation and wood productivity in tropical forests. *Biogeosciences*,
622 13(8), 2537–2562. <https://doi.org/10.5194/bg-13-2537-2016>

623 Waide, R. B., Willig, M. R., Steiner, C. F., Mittelbach, G., Gough, L., Dodson, S. I., Juday, G. P., &
624 Parmenter, R. (1999). The Relationship Between Productivity and Species Richness. *Annual Review of*
625 *Ecology and Systematics*, 30(1), 257–300. <https://doi.org/10.1146/annurev.ecolsys.30.1.257>

626 Wei, W., Weile, C., & Shaopeng, W. (2010). Forest soil respiration and its heterotrophic and autotrophic
627 components: Global patterns and responses to temperature and precipitation. *Soil Biology and Biochemistry*,
628 42(8), 1236–1244. <https://doi.org/10.1016/j.soilbio.2010.04.013>

629 Zak, D. R., Tilman, D., Parmenter, R. R., Rice, C. W., Fisher, F. M., Vose, J., Milchunas, D., & Martin, C.
630 W. (1994). Plant Production and Soil Microorganisms in Late-Successional Ecosystems: A Continental-Scale
631 Study. *Ecology*, 75(8), 2333. <https://doi.org/10.2307/1940888>